East European Journal of Physics. 4. 334-340 (2024)
DOI:10.26565/2312-4334-2024-4-38 ISSN 2312-4334

SCALE MODELING OF THE INFLUENCE OF MULTIPLE LOCALIZED DEFECTS OF METAL SURFACE ON OPTICAL ELLIPSOMETRY RESULTS

Oleksii Haluza[a,b,*], Ivan Kolenov[c,d], Iryna Gruzdo[b]
[a]*National Technical University "Kharkiv Polytechnic Institute", 2 Kyrpychova St., Kharkiv, 61002, Ukraine*
[b]*Kharkiv National University of Radio Electronics, 14 Nauky Ave., Kharkiv, 61166, Ukraine*
[c]*Institute of Electrophysics and Radiation Technologies of NAS of Ukraine, P.B. 8812, 28 Chernyshevsky St., Kharkiv, 61002, Ukraine*
[d]*O.Ya. Usikov Institute for Radiophysics and Electronics of NAS of Ukraine, 12, Ac. Proskura St., Kharkiv, 61085, Ukraine*
**Corresponding Author e-mail: oleksii.haluza@khpi.edu.ua*
Received June 29, 2024; revised September 24, 2024; accepted October 21, 2024

The work is devoted to the problem of ellipsometric studies of real surfaces and considers the case when surface inhomogeneities are individual localized defects or conglomerates with a size comparable to the wavelength of the probing radiation. Such inhomogeneities lead to angular dependences of ellipsometric parameters that have a non-classical form and cannot be described using conventional well-known models of homogeneous planar layers. This work focuses on the influence of conglomerates of localized defects on the angular dependences of ellipsometric parameters and serves as a continuation of earlier studies in which single localized defects were considered. The dependence of the degree of influence of the distance between defects on the ellipsometric parameters is examined. The parameter "critical distance" between defects is introduced, beyond which they can be considered as localized, and estimates of this parameter for the considered configurations are provided.
Keywords: *Ellipsometry, Terahertz waves, Scale modeling, Surface defects, Localized defects*
PACS: 68.35.Ct, 42.25.Ja, 78.68.+m

1.INTRODUCTION

Ellipsometry is a non-contact, precise, non-destructive method for studying the properties of surfaces and interfaces. It is based on measuring changes in the polarization state of radiation after it is reflected from the surface of a sample or passes through a transparent sample [1-3].

In most cases, a pair of parameters, Ψ and Δ (the so-called ellipsometric parameters), is the result of an ellipsometric experiment. The first parameter characterizes the relative change in amplitude ratios, and the second one represents the change in the phase difference of the orthogonal components (p- and s-components) of the electromagnetic wave during their interaction with the system under study. The simplest configuration of an ellipsometric experiment (a scheme with a rotating analyzer, RAE) is shown in Fig. 1. Electromagnetic radiation from the source S passes through a polarizer P with a known azimuth and is reflected from the sample, leading to a change in the polarization state. Next, the radiation passes through another polarizer (the Analyzer), and detector D measures the radiation amplitude. In the RAE scheme, the ellipsometric parameters Ψ and Δ are found from the dependence $I(A)$ of the intensity of the recorded signal on the azimuth of the analyzer A [2, 3].

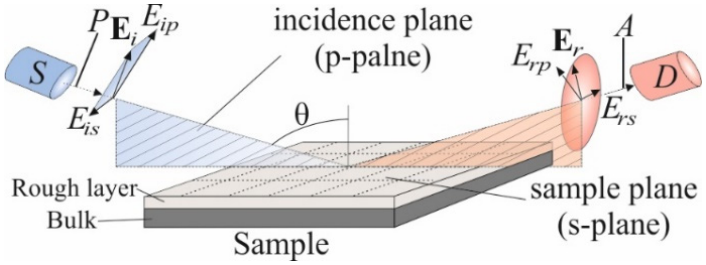

Figure 1. Schematic of the ellipsometric experiment

Ellipsometric parameters are related to the physical characteristics of the structure under study and are related to those measured by the basic equation of ellipsometry:

$$\rho = tg\Psi \cdot e^{i\Delta} = \frac{R_p}{R_s}, \quad (1)$$

where $R_{p(s)}$ are the complex Fresnel coefficients of the sample.

The advantages of ellipsometry include high accuracy and reproducibility of results, as well as the absence of a need for a reference measuring channel or reference sample. These benefits have led to its widespread application in many areas [2, 5-9]. However, ellipsometry is an indirect technique, meaning that to calculate the material characteristics, it is

Cite as: O. Haluza, I. Kolenov, I. Gruzdo, East Eur. J. Phys. 4, 334 (2024), https://doi.org/10.26565/2312-4334-2024-4-38

necessary to solve equation (1) for the desired parameters, which are typically the optical constants of the sample material and/or the optical constants and thickness of film coatings. The exact form of the right-hand side of equation (1) is determined by the physical model chosen to describe the structure under study [1-3, 10, 11]. For analyzing ellipsometric experiments, researchers often use planar surface models, including those of clean surfaces or multilayer systems with distinct boundaries between layers. These models are usually just approximations of real structures, so the development of more accurate models for the structures under study remains one of the main challenges in ellipsometry. A specific problem arises when analyzing ellipsometric data for surfaces with deviations from planarity [12-15], such as roughness (medium and highly rough surfaces), island films, regular reliefs [16, 17], grains in polycrystals, inclusions of secondary phases, blistering, and more [18, 19]. The last three types of structures can be classified as localized defects [20]. Localized defects disrupt the statistical homogeneity of surface properties and are therefore poorly described by effective medium models (which are represented by homogeneous films with averaged optical constants [2, 21]) or random fields with homogeneous statistical properties [22-24]. Since localized defects often appear on real surfaces due to various processes, such as sputtering with high-energy particle beams or chemical etching, analyzing the results of optical studies (e.g., ellipsometry, reflectometry) is highly relevant [18, 19]. It is important to note that there is currently a lack of general understanding regarding how these surface defects impact ellipsometry results [20].

This work is a continuation of [20], which addressed the problem of creating and testing a physical ellipsometric model of localized defects using a sub-terahertz null ellipsometer with an operating wavelength of 2.14 mm. In [20], quasi-optical scale modeling of the influence of a single localized defect (a series of samples with defects of various sizes on a millimeter scale) located at the center of the sample was conducted and analyzed. It was demonstrated that if the size of a localized defect is slightly smaller than the wavelength, ellipsometry does not "see" it, while reflectometry shows a decrease in the reflection coefficient compared to a clean surface. However, conglomerates of defects are much more common in real samples. They can simultaneously affect the change in the polarization state of the probing radiation upon reflection. Therefore, a logical next step in the development of quasi-optical scale modeling is to study the simultaneous influence of multiple defects of various sizes, spaced apart at specified distances. This study focuses on experimentally examining how a group of parallelepiped defects affects radiation scattering, polarization, and the measured ellipsometric parameters. The study also examined the "localization" of defects, i.e., determining the minimum distance at which they begin to independently influence the result of the experiment.

2. EXPERIMENTAL PROCEDURE AND SAMPLES

Since optical ellipsometry operates with wavelengths on the order of half a micrometer, the size of defects that are relevant cannot exceed 1 micrometer and most often have a significantly smaller size. It is clear that artificially and controllably creating such defects with given shapes, sizes, and relative positions on a defect-free surface is currently a technically complex, time-consuming, and expensive task. Therefore, it was decided to take advantage of the property that the features of the interaction of EM radiation with objects are determined not by the absolute values of the radiation wavelength (λ) and the characteristic sizes of objects (d), but by their ratio. In our case, we are interested in ratios in the range $d/\lambda = 0.1$ to 2. To be able to create the desired defects, their size must be about 1 mm. Accordingly, to maintain the specified d/λ ratio, the wavelength must be on the order of several mm (in our case, $\lambda = 2.14$ mm). This allows for the relatively easy creation of surfaces with a preassigned defect geometry and the performance of ellipsometric (and other) measurements, the results of which can be transferred to optical-range ellipsometry. This approach is commonly called "scale modeling" and is often used in radiophysics. However, in radiophysics, reduced models are typically constructed, leading to the use of proportionally smaller wavelengths. This enables the study of the scattering of long-wavelength waves from large objects under laboratory conditions. In our case, we propose to use enlarged models and wavelengths.

To carry out large-scale modeling, in this study, a quasi-optical terahertz ellipsometer (QOTE) operating at a probing radiation wavelength of 2.14 mm (0.14 THz) was used. QOTE is built based on the PCSA (Polarizer – Compensator – Sample – Analyzer) scheme and implements a rotating-analyzer measurement scheme (Rotating Analyzer Ellipsometry, RAE) in an automated mode using specially developed hardware and software. The advantages of this scheme include the relative simplicity of design and measurements, as well as the ability to study both absorbing and transparent materials (due to the presence of a compensator). The measurement error for the ellipsometric parameters Ψ and Δ provided by QOTE is 0.05° and 0.1°, respectively.

QOTE is based on a quasi-optical transmission line - a hollow dielectric beam guide and quasi-optical devices and components for the frequency range 0.1...1 THz, developed at the O. Ya. Usikov Institute of Radiophysics and Electronics NAS of Ukraine [25, 26]. Fig. 2 shows the quasi-optical design of QOTE. The generator (G) signal is output through a standard waveguide and transmitted to the quasi-optical beamguide transmission line via a waveguide-beamguide junction (1). The signal is modulated by a mechanical amplitude modulator (2). The attenuator (3) serves as a linear polarizer in the circuit, allowing adjustment of the probing signal amplitude. The polarization plane rotator (4) rotates the polarization plane by an arbitrary angle P. Thus, in this circuit, the function of a polarizer with a variable azimuth is performed by a pair of elements: the linear polarizer itself (as part of the attenuator) and the polarization plane rotator. Next, compensator (5) converts the radiation into elliptically polarized radiation, adding a controlled phase shift between orthogonally polarized components. The measuring cell, which includes a goniometer with a sample holder, provides the required angle of incidence of radiation θ on the study object S mounted on it. The analyzer function is performed by a

pair of elements: a polarization plane rotator (6), which determines the azimuth of analyzer A, and the fixed angle analyzer itself (7). This design of the analyzer is due to the polarization sensitivity of the detector (D). The signal from the (D) goes to the input of the synchronous detector. After the synchronous detection procedure, the signal is measured using the ADC interface unit, and the result is transmitted to the PC. All rotating elements are equipped with stepper motors and controlled by a PC via a special interface. Measuring the intensity dependence on an azimuth of the analyzer is performed automatically. QOTE is described in more detail in [27].

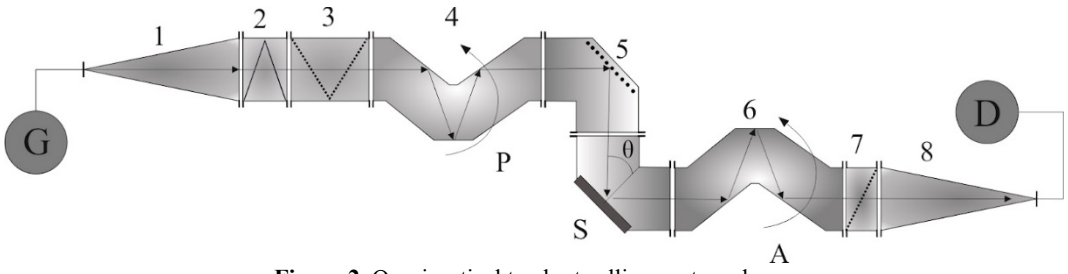

Figure 2. Quasi-optical terahertz ellipsometer scheme

The sample material for this study was Epcos No. 87 ferrite. The choice of material was based on its optical properties (n~6.7, k~4.0) [18, 19], which are similar to those of metals in the optical range.

The samples used in this study were ferrite plates with a size of 50×22×6 mm. Probe beam diameter is 20 mm (Fig. 3(a)). Several identical defects, each in the form of a parallelepiped with dimensions a, b, and c, made of the same material were placed in the center of the plate and beam (Fig. 3(b)). The position of the defects is specified by a single parameter - the distance d from the sample center to the defect.

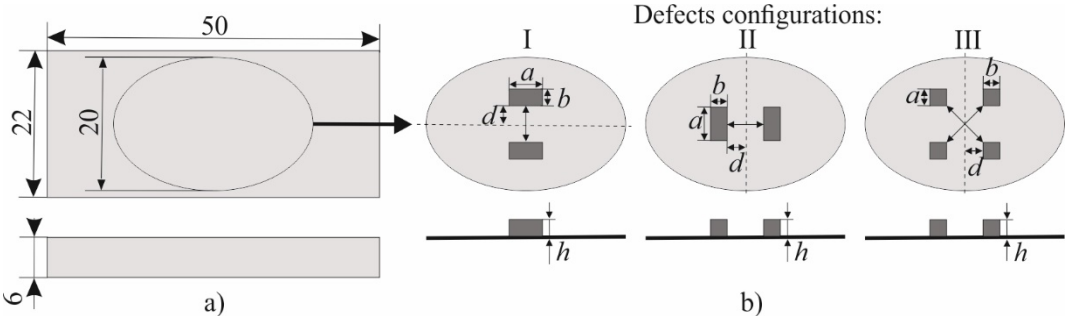

Figure 3. Schematic representation of the sample, the distribution of the beam spot, and the arrangement of defects on the sample surface

For quasi-optical scale modeling of the influence of several defects on ellipsometric parameters, three defect configurations were considered: a) two parallelepipeds with a long side parallel to the plane of incidence, located symmetrically relative to the plane of incidence at a distance of 2d from each other (Fig. 3b), configuration I); b) two parallelepipeds oriented with their long sides perpendicular to the plane of incidence, located symmetrically relative to the center of the sample and spaced at a distance of 2d (Fig. 3b), configuration II); c) four defects, square in plan ($a = b$), with sides parallel to the sides of the sample, located symmetrically at a distance d from its center (Fig. 3b), configuration III). It should be noted that the total defect area is the same in all three configurations.

The ellipsometric parameters Ψ and Δ were measured for surfaces with defects of varying sizes (parameters a, b, and h) and relative positions (parameter d). In configurations I and II, defects with plan dimensions a = 5 mm and b = 2.5 mm, and heights h = 2.5 mm and 1.5 mm were considered. In configuration III, the defects had dimensions $a = b$ = 2.5 mm in plan and three heights h = 2.5 mm, 1.5 mm, and 0.5 mm. The parameter d in all configurations varied from 0 to 12 mm. All options for defect parameters and configurations are summarized in Table 1.

Table 1. Parameters of defects (a, b, h) and their relative position (d) for all configurations.

	***a*, mm**	***b*, mm**	***h*, mm**	***d*, mm**
Configuration I	5.0	2.5	1.5; 2.5	0, 1, 2, 3, 5, 7, 9, 12
Configuration II	5.0	2.5	1.5; 2.5	
Configuration III	2.5	2.5	0.5; 1.5; 2.5	0, 1, 2, 3, 5, 7, 12

The choice of defect parameters and configurations is determined by the results obtained in [20]. As mentioned above, [20] shows that a single defect, with a characteristic size less than the wavelength λ, becomes “invisible” for ellipsometry. If the defect size significantly exceeds λ, then the angular dependences of the ellipsometric parameters become non-trivial. Thus, for the study of multiple defects, defects and their configurations with dimensions comparable

to the wavelength of the probing radiation (in our case, λ = 2.14 mm) are of greatest interest. In addition, it is precisely this range of ratios of defect size to wavelength that is most interesting from the point of view of large-scale modeling of the effect of defects on the results of optical ellipsometry. The goal of the experiment was to clarify the conditions under which defects can be considered localized from the point of view of ellipsometry, i.e., when multiple defects can be considered as individual defects, as a single defect, or as a group of defects influencing each other (i.e., not localized defects). Next, we present the results of the experiment.

3. EXPERIMENTAL RESULTS

Fig. 4 shows the experimental angular dependences of Ψ and Δ for the initial (bare) ferrite surface without defects (dots). From these data, the optical constants of the substrate were determined in the bare surface model [2] (n = 6.74, k = 4.02). The lines in Fig. 4 represent the angular dependences of Ψ and Δ corresponding to these values of optical constants. One can see that the experimental data are described by the model of a bare isotropic surface with an error not exceeding the experimental error. With these optical constants, the probing radiation does not penetrate this material beyond 10 μm. Accordingly, the samples under study can be considered as bulk (without coatings), and the results of further experiments related to the presence of defects on the surface can be interpreted without taking into account interference effects in the defect and/or substrate.

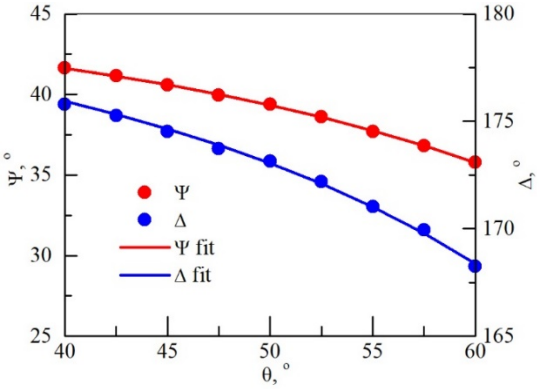

Figure 4. Angular dependencies of the experimental data (dots) and fitted model (lines) for the ellipsometric parameters Ψ and Δ of the defect-free substrate.

Next, we consider part of the experimental results that reflect the general trends in the influence of changes in defect configurations on the ellipsometric parameters Ψ and Δ. Fig. 5 shows the experimental results for defect configurations I (h = 1.5 mm), II (h = 2.5 mm), and III (h = 2.5 mm) as listed in Table. 1. For the convenience of analysis, the figures show the following dependencies of ellipsometric parameters differences:

$$\delta\Psi(\theta) = (\Psi(\theta) - \Psi_0(\theta)), \quad \delta\Delta(\theta) = (\Delta(\theta) - \Delta_0(\theta)), \tag{2}$$

where $\Psi_0(\theta)$ and $\Delta_0(\theta)$ are the ellipsometric parameters of the defect-free surface (see Fig. 4). Thus, the effect of a defect on the ellipsometric parameters relative to a bare surface is illustrated.

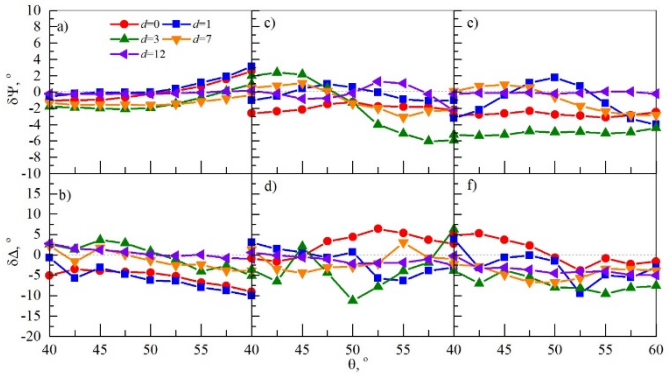

Figure 5. Experimental angular difference dependencies of ellipsometric parameters Ψ (a) and Δ (b) for configurations I (a), b), h = 1.5 mm), II (c), d), h = 2.5 mm), III (e), f), h = 2.5 mm).

Fig. 5 shows that the nature of the dependencies for different configurations is similar. For all configurations with h = 2.5 mm, oscillations of the angular dependencies of the ellipsometric parameters are observed. At h = 1.5 mm, the oscillations have less amplitude. However, despite the different local nature of the dependencies for all configurations, they have similar integral properties. A single large defect (d = 0 mm) causes a significant deviation of the angular

dependencies $\Psi(\theta)$ and $\Delta(\theta)$ from the clean surface. As the distance d between defects increases in all three configurations, both $\Psi(\theta)$ and $\Delta(\theta)$ initially deviate further from the clean surface, but with a further increase in distance, they start to approach the clean surface values. Thus, individual defects in all configurations become "invisible" to ellipsometry as the distance between them increases.

4. ANALYSIS OF RESULTS

From the above graphs, it is difficult to quantitatively estimate the degree of deviation of the $\Psi(\theta)$ and $\Delta(\theta)$ dependencies from the "bare surface" for various defect configurations. Therefore, to characterize the degree of deviation of the angular dependencies for surfaces with and without defects, we will use the arithmetic mean of the root-mean-square differences:

$$\sigma = \frac{1}{2}\left(\sqrt{\frac{1}{n}\sum_{i=0}^{n}(\Psi_{\theta_i}^{bare} - \Psi_{\theta_i}^{def})^2} + \sqrt{\frac{1}{n}\sum_{i=0}^{n}(\Delta_{\theta_i}^{bare} - \Delta_{\theta_i}^{def})^2}\right), \quad (3)$$

where $\Psi_{\theta_i}^{bare}$ and $\Delta_{\theta_i}^{bare}$ are the ellipsometric parameters of a defect-free sample at an angle of incidence θ_i, $\Psi_{\theta_i}^{def}$ and $\Delta_{\theta_i}^{def}$ are the parameters for a sample with defects, and n is the number of measurements at different angles of incidence θ. Next, we consider the dependences $\sigma(d)$ for various configurations and defect height h (Fig. 6).

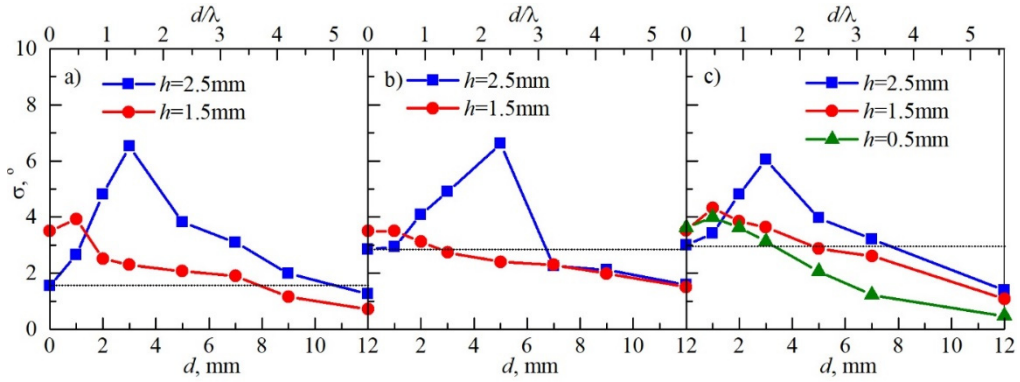

Figure 6. Dependences of σ(d) in configurations I (a), II (b), and III (c) for different defect heights.

Fig. 6 shows that in all 3 configurations, the dependences $\sigma(d)$ at h = 2.5mm (h/λ~1) are qualitatively the same and quantitatively close. Namely, $\sigma(d)$ increases monotonically and reaches a maximum at $d/\lambda \sim 1.5$ (configurations I and II) and $d/\lambda \sim 2$ (configuration II). Further, σ monotonically tends to 0. At h=1.5mm and 0.5mm ($h/\lambda \sim$ ¾, $h/\lambda \sim$ ¼), the dependencies are qualitatively similar, but the maxima are less by value and shifted to the d~1 region.

From the above results, it is clear that the influence of the considered localized defects on the ellipsometric parameters Ψ and Δ is significant and non-trivial. Thus, the presence of various configurations defects leads to a qualitative change like the angular dependencies $\Psi(\theta)$ and $\Delta(\theta)$ compared to a "bare surface". From the experimental data, it is clear that the main influence of defects appears in oscillations of ellipsometric parameters around the clean surface (Fig. 5). This effect is associated with the interference of waves reflected from different areas of the defective surface [15]. It is worth noting that for high defects (h=2.5mm, h/λ~1) the oscillations are greater in amplitude and frequency. As the height of the defects decreases, the oscillations decrease, and for defects with a height of 0.5 mm, they are practically absent.

The results in Fig. 6 can be divided according to the h parameter (2.5, 1.5, and 0.5 mm) because the trends in the $\sigma(d)$ dependencies are similar for different defect configurations. One can see that the $\sigma(d)$ dependencies at h=2.5mm (~1λ) have explicit maxima for all defect configurations at d=3-5 mm (which corresponds to ~1-2λ). So, at a given distance d between defects, the maximum influence of interference effects on the ellipsometric parameters occurs. With a further increase in d, the σ values monotonically decrease, which indicates a decrease in the interaction between defects. Wherein, σ(0)=σ(3.5-4.5λ), i.e. starting from a critical distance d_{cr} = 4.5λ between defects, the defects stop interacting and can be considered as localized.

In the case of defects with a smaller height (h=1.5mm = ~3/4λ and h=0.5mm = ~1/4λ) $\sigma(d)$ is smaller in value, which indicates less interference interaction between defects. At the same time, the dependencies $\sigma(d)$ begin to decrease monotonically starting from σ(0.5λ), which indicates the maximum interaction of defects at a distance of fractions of a wavelength. It is also worth noting that for cases d=(0.5 and 1.5 mm) σ(0)~σ(<1λ) we can conclude that the distance d_{cr} at which defects become localized depends on their dimensions and, firstly, turn from their height. A similar dependence is observed in the case of configuration III at h = 0.5 mm.

We previously observed similar non-classical behavior of ellipsometric parameters in measurements in the optical range (λ = 633 nm) [18] and in large-scale simulations with a single localized defect [20]. In [18], samples of a precipitation-hardened copper alloy were studied and subjected to radiation sputtering, which led to the appearance of a

significant number of localized defects (Fig. 7), specifically harder particles of secondary phases. In this work, the angular dependences $\Psi(\theta)$ and $\Delta(\theta)$ were obtained for the first time, with their profiles being radically different from the classical ones. Additionally, a hypothesis was formulated that explained this behavior as being due to the presence of localized defects, and predicted that if the size of such a defect is several times smaller than the wavelength, ellipsometry would cease to be sensitive to these defects.

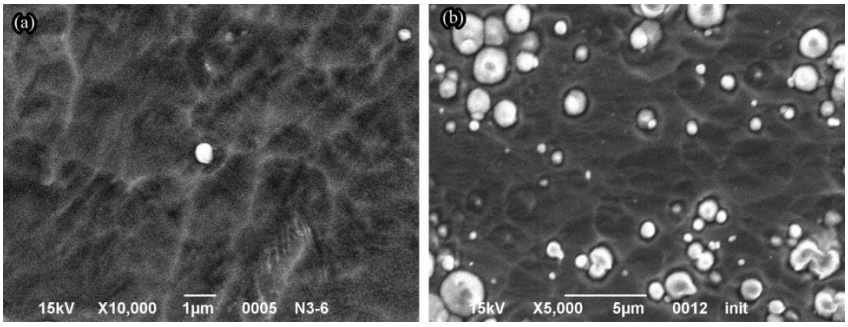

Figure 7. Examples of localized surface defects in a sputtered precipitation-hardened CuCrZr alloy: (a) single defect and (b) multiple defects

The results of this work confirm this hypothesis. Specifically, it is shown that the behavior of the angular dependences Ψ(θ) and Δ(θ) is linked to the presence of localized defects whose size is several times larger than the wavelength of the probing radiation. As the size of the localized defects decreases and the degree of localization increases (i.e., the distance between defects in the case of grouped defects) to sizes slightly smaller than the wavelength of the probing radiation, the defects become "invisible" to ellipsometry but continue to significantly influence specular reflection.

5. CONCLUSIONS

Thus, the work demonstrates that deviations from the classical behavior of the angular dependences of the ellipsometric parameters are grounds to assume the presence of localized defects or their conglomerates. In this case, statistically homogeneous defect layers (such as roughness, transition layers, etc.) never lead to qualitative deviations from the classical behavior of angular dependencies.

It is also shown that for all defect configurations studied, with small distances between defects, they have a joint effect on the ellipsometry results. At a certain distance, defects begin to influence ellipsometry results independently. Accordingly, a critical distance for defect localization can be introduced, beyond which they do not jointly affect the ellipsometric parameters. So, for $h/\lambda \sim 1$, d_{cr} is equal to 3.5-4.5λ; for $h/\lambda \sim ¾$ and ¼ - less than λ. Thus, d_{cr} decreases with decreasing h/λ ratio. The detailed form of the $d_{cr}(h/\lambda)$ dependence will be investigated in a separate study.

As mentioned above, defects of relatively large sizes (~λ) can lead to oscillations in the angular dependences of ellipsometric parameters, which can be used to determine the characteristics of roughness. As the defect height h decreases, the oscillation period increases; therefore, to more thoroughly study the influence of defects with $h < 0.7\lambda$, measurements in a larger range of incidence angles are required.

Acknowledgments

The research presented in this article was financially supported by the Simons Foundation Program: Presidential Discretionary-Ukraine Support Grants, Award No 1030287.

ORCID

Oleksii Haluza, https://orcid.org/0000-0003-3809-149X; **Ivan Kolenov,** https://orcid.org/0000-0002-1741-5195
Iryna Gruzdo, https://orcid.org/0000-0002-4399-2367

REFERENCES

[1] R.M.A. Azzam, and N.M. Bashara, *Ellipsometry and polarized light* (North Holland, Amsterdam, 1999).
[2] H. Fujiwara, *Spectroscopic Ellipsometry: Principles and Applications* (Wiley, Chichester, 2007).
[3] H.G. Tompkins, and W.A. McGahan, *Spectroscopic Ellipsometry and Reflectometry: A User's Guide* (Wiley, Chichester, 1999).
[4] S. Zollner, F. Abadizaman, C. Emminger, and N. Samarasingha, Adv. Opt. Technol., **11**, 117 (2022), https://doi.org/10.1515/aot-2022-0016
[5] B. Hajduk, H. Bednarski, and B. Trzebicka, J. Phys. Chem. B, **124**(16), 3229 (2020). https://doi.org/10.1021/acs.jpcb.9b11863
[6] S. Bairagi, C.-L. Hsiao, R. Magnusson, J. Birch, J.P. Chu, F.-G. Tarntair, R.-H. Horng, K. Järrendahl, Opt. Mater. Express, **12**, 3284 (2022), https://doi.org/10.1364/OME.462668
[7] M.S. Gangwar, P. Agarwal, Phys. Scr. **98**, 105944 (2023). https://doi.org/10.1088/1402-4896/acf796
[8] W. Leigh, S. Mandal, J.A. Cuenca, D. Wallis, A.M. Hinz, R.A. Oliver, E.L.H. Thomas, and O. Williams, ACS Omega, **8**, 30442 (2023). https://doi.org/10.1021/acsomega.3c03609
[9] K. Ungeheuer, K.W. Marszalek, M. Mitura-Nowak, *et al*., Sci Rep. **13**, 22116 (2023). https://doi.org/10.1038/s41598-023-49133-x
[10] A. Lemire, K. Grossklaus, T.E. Vandervelde, IEEE Dataport, (2024). https://dx.doi.org/10.21227/xhrd-ny57

[11] D. Schmidt, E. Schubert, and M. Schubert, in: *Ellipsometry at the Nanoscale*, edited by M. Losurdo and K. Hingerl (Springer Berlin Heidelberg, 2013), pp. 341-410.
[12] S. Bian, and O. Arteaga, Opt. Express, **31**(12), 19632-19645 (2023). https://doi.org/10.1364/oe.490197
[13] W. Yu, C. Cui, H. Li, S. Bian, and X. Chen, Photonics **9**(9), 621 (2022), https://doi.org/10.3390/photonics9090621
[14] N.C. Bruce, O.G. Rodríguez-Herrera, C.N. Ramírez, and M. Rosete-Aguilar, Appl. Opt. **60**(5), 1182 (2021). https://doi.org/10.1364/AO.410003
[15] T. V. Vorburger, and K. C. Ludema, Appl. Opt. **19**(4), 561 (1980). https://doi.org/10.1364/AO.19.000561
[16] M.G. Tchéré, S. Robert, J. Dutems, H. Bruhier, B. Bayard, Y. Jourlin, and D. Jamon, Appl. Opt. **63**(14), 3876 (2024). https://doi.org/10.1364/AO.520109
[17] G.G. Politano, and C. Versace, Spectrosc. J. **1**(3), 163 (2023). https://doi.org/10.3390/spectroscj1030014
[18] A.I. Belyaeva, A.A. Galuza, P.A. Khaimovich, *et al*., Phys. Metals Metallogr. **117**, 1170 (2016). https://doi.org/10.1134/S0031918X16090027
[19] A.I. Belyaeva, V.Kh. Alimov, A.A. Galuza, K. Isobe, V.G. Konovalov, I.V. Ryzhkov, A.A. Savchenko, *et al*., J. Nucl. Mater. **413**(1), 5 (2011), https://doi.org/10.1016/j.jnucmat.2011.03.026
[20] A.I. Belyaeva, A.A. Galuza, V.K. Kiseliov, I.V. Kolenov, A.A. Savchenko, Ye.M. Kuleshov, and S.Yu. Serebriansky, Telecommunications and Radio Engineering **74**(2), 171 (2015). https://doi.org/10.1615/TelecomRadEng.v74.i2.60
[21] N.L. Dmitruk, A.V. Goncharenko, and E.F. Venger, *Optics of Small Particles and Composite Medi*a, (Naukova Dumka, Kyiv, 2009).
[22] O.V. Angelsky, and P.P. Maksimyak, Optical Engineering, **34**(4), 973 (1995). https://doi.org/10.1117/12.197181
[23] X. Liu, Q. Chen, J. Zeng, Y.J. Cai, and C.H. Liang, Opto-Electron Sci. **2**, 220024 (2023). https://doi.org/10.29026/oes.2023.220024
[24] M. W. Hyde, J. Opt. Soc. Am. A, **39**(12), 2383 (2022). https://doi.org/10.1364/JOSAA.465457
[25] S. Mizrakhy, in: *IEEE First Ukraine Conference on Electrical and Computer Engineering* (UKRCON, Kyiv, Ukraine, 2017), pp. 198-201, https://doi.org/10.1109/UKRCON.2017.8100473
[26] I.A. Tishchenko, and A.I. Nosich, IEEE Microw. Mag. **4**(4), 32 (2003), https://doi.org/10.1109/MMW.2003.1266065
[27] A.A. Galuza, V.K. Kiseliov, I.V. Kolenov, A.I. Belyaeva, and Y.M. Kuleshov, IEEE Trans. THz Sci. Technol. **6**(2), 183 (2016), https://doi.org/10.1109/TTHZ.2016.2525732

МАСШТАБНЕ МОДЕЛЮВАННЯ ВПЛИВУ МНОЖИННИХ ЛОКАЛІЗОВАНИХ ДЕФЕКТІВ ПОВЕРХНІ МЕТАЛУ НА РЕЗУЛЬТАТИ ОПТИЧНОЇ ЕЛІПСОМЕТРІЇ

Олексій Галуза[a,b], Іван Коленов[c,d], Ірина Груздо[b]

[a]Національний технічний університет «Харківський політехнічний інститут», вул. Кирпичова, 2, м. Харків, 61002, Україна
[b]Харківський національний університет радіоелектроніки, пр. Науки, 14, м. Харків, 61166, Україна
[c]Інститут електрофізики і радіаційних технологій НАН України, вул. Чернишевського, 28, м. Харків, 61002, Україна
[d]Інститут радіофізики та електроніки ім. О.Я. Усикова НАН України, вул. Ак. Проскури, 12, 61085, м. Харків, Україна

Робота присвячена проблемі еліпсометричних досліджень реальних поверхонь і розглядає випадок, коли поверхневі неоднорідності являють собою окремі локалізовані дефекти або їх конгломерати розміром, порівняним з довжиною хвилі зондуючого випромінювання. Такі неоднорідності призводять до кутових залежностей еліпсометричних параметрів, які мають некласичний вигляд і не можуть бути описані за допомогою звичайних відомих моделей однорідних плоских шарів. Ця робота присвячена вивченню впливу конгломератів локалізованих дефектів на кутові залежності еліпсометричних параметрів і є продовженням попередніх досліджень, у яких розглядалися поодинокі локалізовані дефекти. Досліджено залежність ступеня впливу відстані між дефектами на еліпсометричні параметри. Введено параметр «критична відстань» між дефектами, за межами якого їх можна вважати локалізованими, та наведено оцінки цього параметра для розглянутих конфігурацій.

Ключові слова: *еліпсометрія; терагерцеві хвилі; масштабне моделювання; поверхневі дефекти; локалізовані дефекти*